The Journal of the Oceanological Society of Korea
Vol. 22, No. 1, p. 25-33, March 1987.

A numerical analysis of sediment transport in an estuary

See Whan Kang, Carl K. Ziegler ** and Wilbert Lick***

* Korea Ocean Research and Development Institute, P.O. Box 29, Panwol Ind. 171-14, Korea

** Department of Mechanical & Environmental Engineering, University of California, Santa Barbara, California 93106

河口隣接 內灣의 堆積物 輸送에 대한 数値모델 解釋

姜始桓* · 카알지글러** · 윌버트릭**

*해양연구소 해양환경공학연구실

**캘리포니아대학 기계 · 환경공학과

Abstract

The transport and fate of fine-grained, cohesive sediments in an estuary were investigated numerically. A numerical model of sediment entrainment, deposition, and transport has been developed by incorporating recent results of laboratory and field investigations.

The time-dependent flow fields produced by river inflow and semi-diurnal tides, were calculated, and the corresponding distributions of suspended-sediment concentrations were obtained. The time-changes of sediment bed condition due to entrainment and deposition were obtained. The entrained sediments contribute initially to high sediment concentrations in the estuary basin. As the time passes, the suspended-sediment concentrations were much reduced by the seaward transport due to residual currents. The erosional and depositional areas were appeared to be strongly dependent on the current-velocity fields and sediment properties of the estuary.

要約 : 河口의 인접한 內灣에서 海流에 의한 微細粒 堆積物質의 輸送, 擴散現象을 数値的으로 分析하였다. 사용된 모델은 水理実験과 現場觀測의 최근 研究決果를 근거로 開発되었으며, 堆積物의 浮上, 堆積, 輸送過程을 보다 실제 상황에 근접하도록 数値 計算하였다. 江의 흐름과 潮汐에 의한 海水流動, 이에 따른 沿岸海域에서의 浮遊物質 濃度, 海底侵食, 그리고 堆積分布에 대한 時間別 変化를 計算하였다. 初期에는 浮上된 堆積物에 의해 浮遊物質의 濃度가 크게 增加되었으나, 時間이 경과됨에 따라 外海로 輸送되어 江河口에서는 濃度가 크게 줄어들었다. 河口隣接 內灣의 海底 堆積物의 侵食과 堆積狀態는 內灣의 地形的 條件에 따른 海流의 流速分布와 堆積物特性에 의해 주로 決定됨을 나타내었다.

INTRODUCTION

Enormous transport of the suspended sediments has been observed off the west coast of Korea, i.e., in the southeastern part of the Yellow Sea. Recent satellite data and field observations (Wells and Huh, 1984; Wells, et al., 1984; Park, et al., 1986) show that the sediment concentrations of the coastal mudstream which flowed southward along the west coast, were very high up to 250mg/ℓ, and they were formed as a band of turbidity front in 25-50km offshore. These suspended sediments were transported into the Korea Straight by the coastal currents.

A major fraction of the sediments in the west coastal areas of Korea are fine-grained, and most of them are derived from the major rivers

(the Han, Keum and Yeongsan) which provide an enormous source for silt and clay particles. The suspended sediments discharged from the rivers are deposited in the estuaries and near-shore areas forming as a series of the mudflats which are commonly found in the west coastal areas. These mudflats serve as a temporary storage of the fine-grained sediments during summer accumulation replenished by extremely high river inflow, and also as a resuspended-sediment source during winter storm (Wells, Park and Choi, 1984). The fine-grained, cohesive sediments in the estuaries are transported seaward through the frequent cycles of resuspension, deposition, and transport by strong tidal currents (up to 3 knots) in the west coast.

These fine-grained sediments have relatively large surface to mass ratios compared to coarse-grained sediments and therefore many contaminants are readily absorbed onto fine-grained sediments and are transported with them. Because of these absorptive capacities, bottom sediments are a major repository of contaminants such as phosphates, heavy metals, and toxic hydro-carbons, and they serve as a highly variable source or sink for contaminants in the overlying water. A quantitative knowledge of the resuspension, deposition and transport of fine-grained sediments is essential in understanding and predicting the fate of contaminants in coastal waters and also heavy sedimentations in navigational channels to reduce dredging costs.

In the present study, a numerical model of the resuspension, deposition, and transport of fine-grained, cohesive sediments has been developed and applied to a typical estuary case. The model is quite general and can treat variable geometry and bottom depth as well as a wide range of boundary conditions. An essential part of this model is an accurate and physically realistic description of the sediment bed and the resuspension and deposition processes occuring at the sediment-water interface due to currents, tides, and wave action. The description of the sediment bed is based on recent experimental and field results for fine-grained, cohesive sediments (Lee, et al., 1981; Lick, 1982; Kang, 1983; Lick and Kang, 1986; MacIntyre, et al., 1986; Massion, et al, 1987; Tsai and Lick, 1987). From these experimental and field results, it is known that at a particular stress the entrainment rate decreases with time such that only a fixed amount of sediment can be entrained over a long period of time. This is in contrast to non-cohensive sediments where the entrainment rate is approximately constant with time. The erosional rates and the net amount of material that can be entrained have been determined as a function of applied shear stress and time after deposition.

GOVERNING EQUATIONS

The sediment transport model has been formulated by the governing equations of hydrodynamics, sediment transport, and sediment flux at the sediment-water interface. The transport of suspended sediment is governed by a three-dimensional convection-diffusion equation. The hydrodynamic equations that must be solved are the three-dimensional conservation of mass and momentum equations for an incompressible, viscous fluid. In order to simplify the equations for shallow water, the following assumptions were made:

1) the pressure varies hydrostatically
2) the Coriolis acceleration is negligible
3) the water column is thoroughly mixed in the vertical direction due to the shallow depth of the water
4) the horizontal velocities and the suspended sediment concentrations are approximately constant in the vertical direction

With these assumptions, the hydrodynamic and sediment transport equations can be reduced from a three-dimensional problem to a two-dimensional problem in the horizontal plane.

Hydrodynamics

The equations that describe the motion of

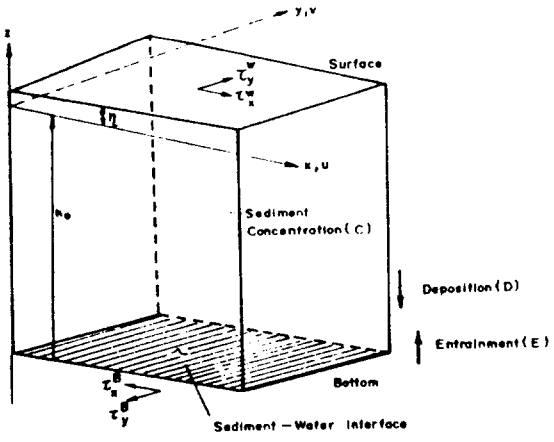

Fig. 1. Definition sketch.

a viscous, incompressible fluid are the conservation of mass and momentum equations. The vertically integrated equations of motion for shallow water are derived as

$$\frac{\partial \eta}{\partial t}+\frac{\partial U}{\partial x}+\frac{\partial V}{\partial y}=0 \tag{1}$$

$$\frac{\partial V}{\partial t}+gh\frac{\partial \eta}{\partial y}=A_H\left(\frac{\partial^2 V}{\partial x^2}+\frac{\partial^2 V}{\partial y^2}\right)+\tau_y^W - \tau_y^B-\frac{\partial}{\partial x}\left(\frac{UV}{h}\right)-\frac{\partial}{\partial y}\left(\frac{V^2}{h}\right). \tag{2}$$

$$\frac{\partial U}{\partial t}+gh\frac{\partial \eta}{\partial x}=A_H\left(\frac{\partial^2 U}{\partial x^2}+\frac{\partial^2 U}{\partial y^2}\right)+\tau_x^W - \tau_x^B-\frac{\partial}{\partial x}\left(\frac{U^2}{h}\right)-\frac{\partial}{\partial y}\left(\frac{UV}{h}\right) \tag{3}$$

in which the notations (see Fig. 1) are

$h=h_o+\eta$: the total water depth
h_o : the equilibrium water depth
η : the surface displacement
U, V : the vertically integrated velocities
A_H : the horizontal eddy viscosity
τ_x^W, τ_y^W : the wind stress at the surface $(z=\eta)$
τ_x^B, τ_y^B : the bottom stress $(z=-h)$

The wind stress is a specified quantity while the bottom stress is calculated using the formular:

$$\tau_x^B=c_f\rho\, U|U| \tag{4}$$

where c_f is a friction factor, and ρ is the water density.

Sediment Transport

The basic equation describing sediment transport is the mass balance or conservation equation. The sediment concentration will be assumed to be approximately independent of z and have no effect on the fluid flow. The vertically integrated sediment transport equation is derived as

$$\frac{\partial (hC)}{\partial t}+\frac{\partial (UC)}{\partial x}+\frac{\partial (VC)}{\partial y}=hD_H\left(\frac{\partial^2 C}{\partial x^2}+\frac{\partial^2 C}{\partial y^2}\right)+q_s+Sh \tag{5}$$

in which the notations are

C : the sediment mass concentration
D_H: the horizontal eddy diffusivity
S : a source term due to reactions in the water
q_s : the sediments flux at the sediment — water interface given by

$$q_s=\left(CW_s-D_v\frac{\partial C}{\partial z}\right)_{z=-h_o} \tag{6}$$

where W_s is the settling velocity of the sediment and D_v is the vertical eddy diffusivity.

The values of h, U, and V are determined from the hydrodynamic equations. In the derivation of the above equation, it has been assumed that the horizontal eddy diffusivity, D_H is constant. The source term S is due to changes in particle size caused by aggregation and disaggregation of sediment particles. A quantitative analysis of sediment transport must consider the fact that sediments consist of a mixture of particles with widely varying size and composition. This distribution of sediment properties can be approximated by separating the sediments into components with each component described by its own average quantities. The above equations are then valid for each component. The quantities S, W_s, and q_s all depend on the state of flocculation of the

sediments. However, neither the rates of flocculation nor the parameters on which flocculation depends are well understood at the present. Because of this, the dynamic effects of flocculation are ignored in the present model and each particle size is considered to be independent of the other particle sizes.

Sediment Flux at the Sediment-Water Interface

The net flux of sediment at the sediment-water interface, denoted by q_s, can be written as the difference between the entrainment (resuspension) rate E and the deposition rate D (Fukuda and Lick, 1980; Lee et al., 1981; Lick and Kang, 1986);

$$q_s = E - D \tag{7}$$

Here the assumption has been made that entrainment and deposition are independent processes, i.e., E is the sediment flux when no suspended sediment and therefore no deposition is present, while D is the sediment flux in the absence of entrainment. In the steady state, $q_s = 0$, and the above equation indicates that there is a dynamic equilibrium at the sediment-water interface between entrainment and deposition.

For sediments of uniform size, a reasonable assumption for this quantity is that it is proportional to the concentration, i.e., $D = \beta C$, where β is a coefficient with units of velocity. Near the sediment-water interface, the significant processes that affect the transport of particles are turbulent diffusion, settling, and Brownian motion. By considering these processes, Lick (1982) determined β as a function of particle size and shear stress. The variation of β with particle size is shown in Figure 2. For small particles less than about 1 μm, values of β are primarily determined by diffusion (both Brownian and turbulent), whereas for larger particles, β is primarily dependent on settling and is approximately equal to the settling velocity W_s. In the natural fine-grained sediment sample found in the near-shore of ocean,

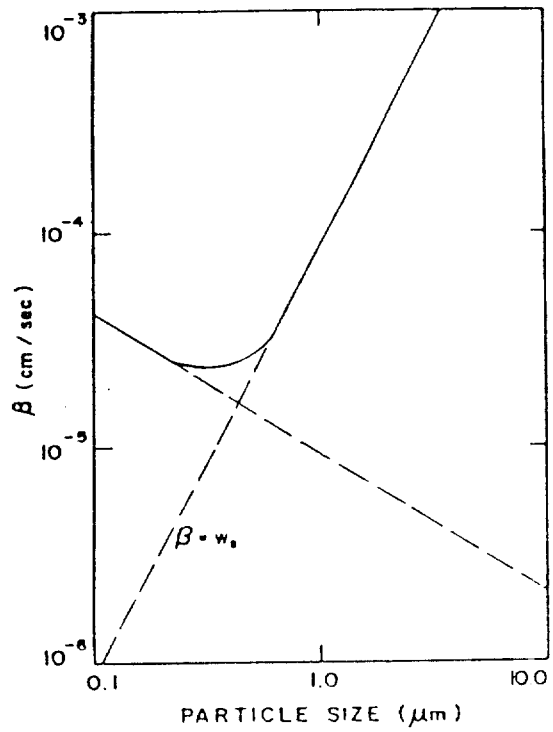

Fig. 2. Deposition parameter β as a function of particle size (after Lick, 1982).

particle sizes and hence settling velocities vary over several orders of magnitude. The deposition rate can be approximated as

$$D = \sum_m \beta_m C_m \tag{8}$$

where the sediments are separated into different components each with its own average particle size, settling velocity and β.

The description of entrainment is relatively simple for sediments consisting of non-cohesive particles of uniform size and properties. In this case, the entrainment rate E is only a function of particle size and applied stress (Massion et al., 1987). The total amount of material entrained for a given shear stress can be written as

$$\varepsilon \equiv \int_0^{\Delta t} E\,dt. \tag{9}$$

For real (especially fine-grained) sediments, the effect on E of particle size variations and

cohesion between particles is significant. At low stresses, only the finer particles on the surface of sediment bed can be entrained while the larger particles are left behind and armor the bed. At any particular stress, this allows only a finite and relatively small amount of sediment to be entrained, i.e., ε is finite as Δt goes to infinity as opposed to non-cohesive, uniform-size sediments where ε is infinite. This is the major difference between idealized, non-cohesive sandy sediments and real, fine-grained sediments. At higher stresses, the larger particles can be entrained and this releases the underlying finer particles. But still only a finite amount of material can be entrained at any particular stress. The entrainment process is further complicated by cohesion of particles and compaction of the bed. These vary with time after deposition and with depth and cause the entrainment rate to vary with time after deposition and depth, e.g., the sediments near the surface are less compacted and relatively easy to entrain while sediments further down are more compacted and more difficult to entrain.

As a first approximation based on recent experimental data and fine-grained sediments (Lee et al., 1981; Kang, 1983; Lick and Kang, 1986; Tsai and Lick, 1987), the following formula for net entrainment is proposed:

$$\varepsilon = a\left[\frac{\tau - \tau_{cr}}{\tau_{cr}}\right]^m \quad \text{for } \tau > \tau_{cr} \tag{10}$$

$$= 0 \quad \text{for } \tau < \tau_{cr}$$

where $$a = a_0/t_d^n \tag{11}$$

and ε is the net amount of entrained sediments/cm^2 of sediment surface, both n and m are approximately equal to two, τ is the shear stress (dynes/cm^2) produced by currents, tides and wave actions, τ_{cr} is the critical shear stress in the order of 1~2 dyne/cm, t_d is the time after deposition in days, and a is approximately 8×10^{-3} for fine-grained sediments but its exact value depends on the particular sediments.

NUMERICAL MODELING OF AN ESTUARY

Finite difference equations which were derived using a volume integral method have been used to approximate the hydrodynamic and sediment transport equations. A volume element is constructed about a grid point in x-y-t space (Fig. 3a). The use of different types of elements make treatment of boundary conditions fairly easy even though a rectangular, uniform grid is used: A full element is used for interior points (Fig. 3b) and three different types of elements are used for boundary conditions; a 1/4 element for 90 degree corners, a 1/2 element for straight boundaries and a 3/4 element for 270 degree corners (Figs. 3c, d, e). The finite difference equations resulting from this method were written in elsewhere (Ziegler and Lick, 1986) and the following results were obtained: (1) explicit, two-time level equations; (2) second-order accuracy in time and space; (3)

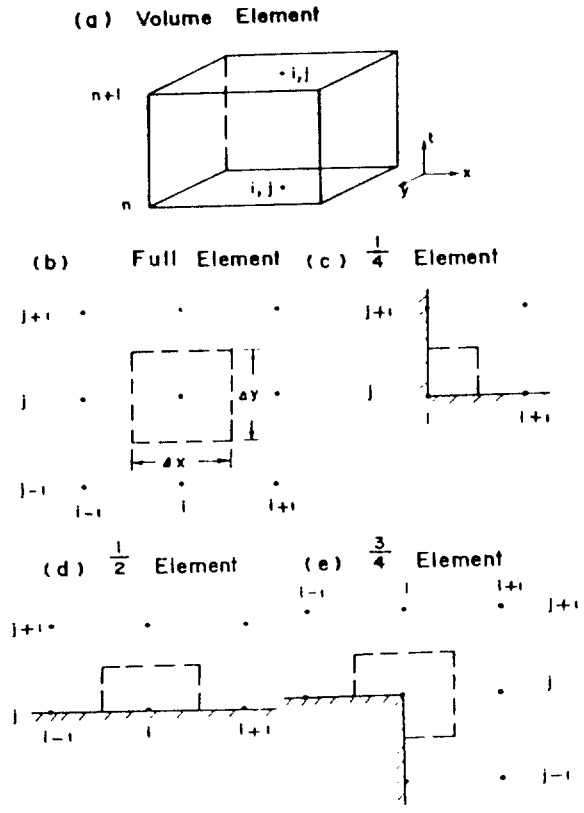

Fig. 3. Computational grid elements: (a) volume element, (b) full element, (c) 1/4 element, (d) 1/2 element, (e) 3/4 element.

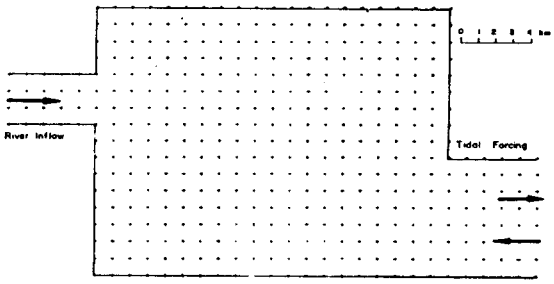

Fig. 4. Numerical grid for the estuary with river inflow and tide.

mass and momentum are conserved locally and globally; (4) boundary conditions are treated properly, especially for open boundary conditions i.e., waves pass through the boundary with minimal numerical reflection and distortion ($\leq 1\%$).

The numerical model of sediment transport in shallow water was used to simulate the processes of sediment resuspension, transport, and deposition in an estuary. Numerical experiments were conducted to examine the transport and fate of fine-grained, cohesive sediments caused by river inflow and tide. The computational grid boundary and areas (17km × 31km) of the estuary are shown in Fig. 4. A constant depth of 20 meters was assumed. Time varying water levels were introduced at the open boundary of estuary entrance:

$$\eta = A_1 \cos(\omega_1 t - \phi_1) + A_2 \cos(\omega_2 t - \phi_2) \quad (12)$$

where $A_1 = 100$ cm, $A_2 = 60$ cm
$\omega_1 = 2.236 \times 10^{-5}$ cycle/s, $\omega_2 = 2.314 \times 10^{-5}$ cycle/s,
$\phi_1 = 235°$, $\phi_2 = 251°$

The tidal forcing at the open boundary varied semi-diurnally and the tidal constituents to use were equivalent to M2 and S2 tides observed in the Nakdong River estuary (Fig. 5). In order to produce strong tidal currents in the estuary, the tidal amplitudes were two times larger than the magnitude observed in the Nakdong River estuary. The maximum tidal-current velocity at the entrance was 113 cm/s.

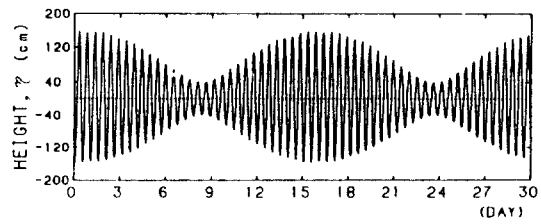

Fig. 5. Tidal forcing at the open boundary of the estuary.

The river-inflow condition was set at a discharge velocity of 20 cm/s, and the sediment concentration of the river inflow was assumed to be a constant value of 100mg/ℓ. A single particle size of 10 microns with $\beta = 10^{-2}$ cm/s was assumed. The initial structure of the sediment bed in the estuary was separated into three layers each of which has different average time after deposition: (1) The First (top) layer; T = 4mm, t_d = 1day (2) The Second layer; T = 4mm, t_d = 2days (3) The Third layer; T = 100mm, t_d = 3days. Here, T is the layer thickness and t_d is the time after deposition or the sediment consolidation time.

The stability criterion for the hydrodynamic equations was approximately determined by numerical experiments (Ziegler and Lick, 1986) as

$$\frac{c\Delta t}{\Delta x} \leq 0.63 \quad (13)$$

where c is the local wave speed, $\Delta x = \Delta y$ is the spatial grid spacing, and Δt is the time interval of the model computation. The same stability criterion applies to the sediment transport equation except that the wave speed c is replaced by the maximum current velocity ($\bar{U}m$) in the flow field. In addition to that, the stability for the sediment transport equations requires the cell Reynolds number

$$Rec = \frac{\bar{U}_m \Delta x}{D_H} \leq 20 \quad (14)$$

Numerical parameters used in the model calculations were as follows: $\Delta x = \Delta y = 1000$m,

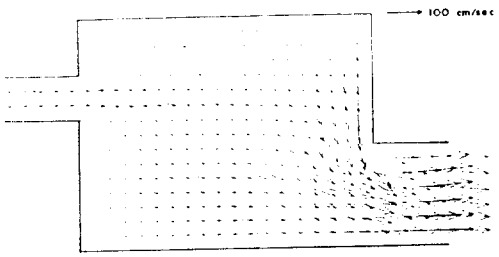

Fig. 6. Ebb currents computed for a Spring tide.

$\Delta t = 45s$, $A_H = 5 \times 10^5$ cm^2/s, $D_H = 5 \times 10^6$ cm^2/s, $C_f = 0.002$, $a = 0.0075$, and $\tau_{cr} = 2$ dynes/cm^2. The currents were allowed to reach a steady-state and then the sediment concentration of the river inflow was raised to a constant value of 100mg/ℓ. Deposition and entrainment of the sediment were also assumed to begin when the flow fields had reached steady-state.

NUMERICAL RESULTS

The ebb and flood flow fields computed for a Spring tide are shown in Figures 6 and 7. The ebb currents were rather stronger than the flood currents in the estuary. The ebb-current velocity of $\geqslant$100 cm/s was found in the estuary entrance channel, particularly the near-shore areas in which the flows were merged into the narrow channel. In the near-shore regions of the boundary corners, the current velocities were very weak in less than 10 cm/s. The flood currents in the basin were generally weak compared to the ebb current. The relatively strong flood-currents ($\sim$20 cm/s) were found in the river mouth and the entrance channel area. The distributions of the suspended-sediment concentrations at 6, 20, and 48 hours after river discharge are shown in Figures 8a, 8b and 8c, respectively. The corresponding contour plots of bottom-sediment thickness are shown in Figures 9a, 9b, and 9c. It can be seen that entrainment and deposition processes were occurred in the estuary basin. Eroded areas are denoted by a negative sediment thickness on the plots while depositional areas have a positive sediment thickness. The zero thickness contour shows the initial position of the top sediment layer.

For the initial 6 hours starting from the ebb to the flood, the entrained sediment contributes

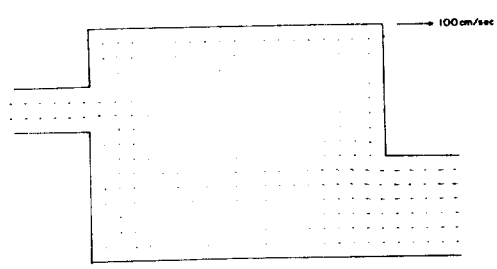

Fig. 7. Flood currents computed for a Spring tide.

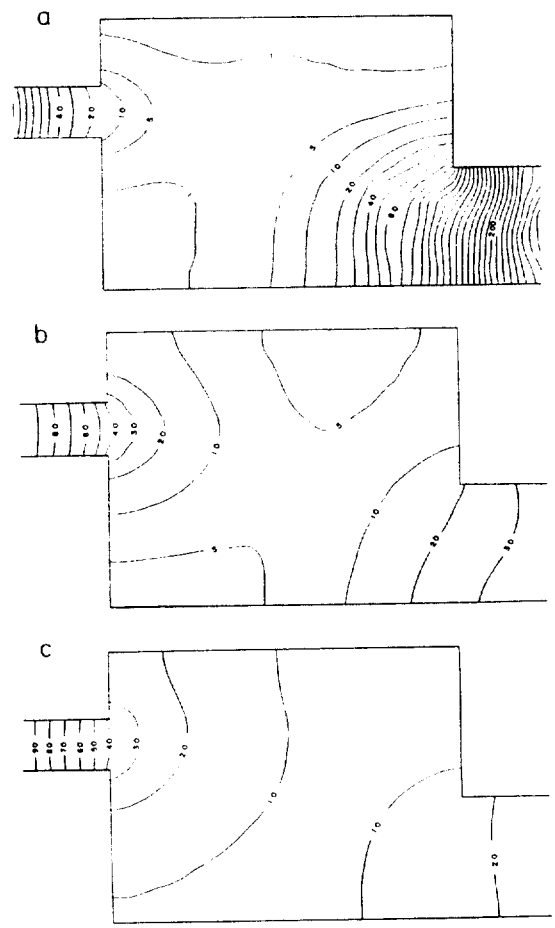

Fig. 8. Distributions of suspended-sediment concentration (mg/ℓ):
(a) t = 6 hours, (b) t = 20 hours, (c) t = 48 hours.

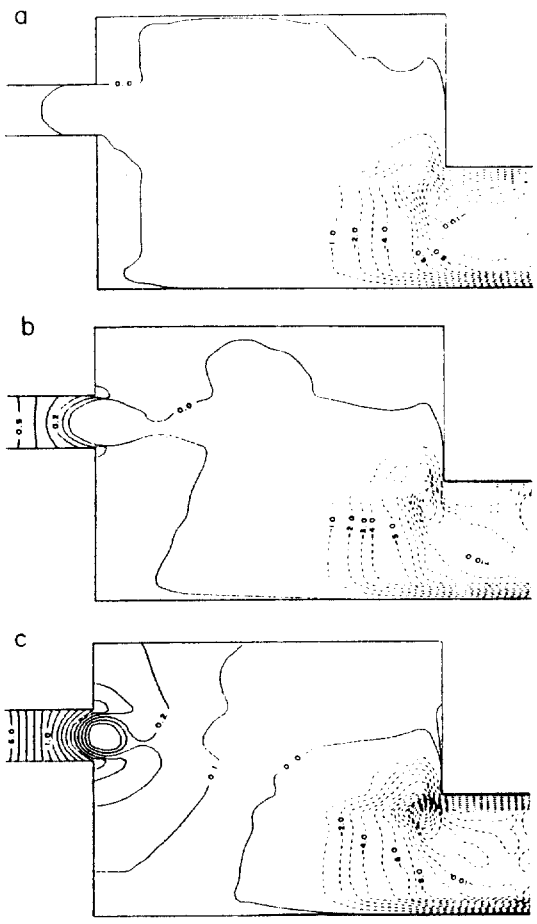

Fig. 9. Distributions of bottom-sediment thickness(mm):
(a) t = 6 hours, (b) t = 20 hours, (c) t = 48 hours.

to the high concentrations of the suspended sediments in the entrance channel areas. The top two-layer sediments of 8mm-thickness have been already entrained and resuspended into the overlying waters. The maximum eroded sediment thickness is -12.8mm and it occurred in the merged areas of the entrance channel. The other erosional area begins as the river enters into the estuary basin. The suspended sediments have been deposited in the river channel and the boundary corner areas of the estuary basin. Figs. 8b and 9b show the sediment concentrations and the contour plot of bottom-sediment thickness at 20 hours. As time passes, the suspended sediments were carried out seaward by the residual currents and thus the concentrations in the basin were gradually reduced. After 20 hours, the distributions of the concentration and the sediment thickness were changed very slowly with time. Figures 8c and 9c show these distributions after 48 hours. The most difference between the time period of 20 and 48 hours is the increase of sediment concentration in the middle of the basin due to dispersion of the suspended sediments discharged from the river. The sediment concentrations in the entrance channel were much reduced by the seaward transport due to the residual current. The maximum eroded sediment thickness after 48 hours is – 19.3mm, and the entrainment rates were getting slower as the entrainment occurred in the deeper layers of the sediments which were more compacted and then hard to be eroded. The maximum sediment deposition after 48 hours is 1.73mm and it occurred in the river channel where the suspended sediments were continuously supplied by the river inflow, and much of them were deposited immediately.

SUMMARY AND CONCLUDING REMARKS

The transport and fate of fine-grained, cohesive sediments in an estuary have been obtained quantitatively through a numerical model of the resuspension, deposition, and transport of the sediments (or contaminants) in shallow water. The model presented here has been developed through much of our present knowledge of the transport of fine-grained, cohesive sediments. This has involved laboratory and field investigations as well as theoretical and numerical modeling. A unique feature of this model is physically more realistic description of the sediment bed and the resuspension processes occurring at the sediment-water interface due to currents, tides, and wave action.

The numerical results show that the sediments entrained by strong shear currents con-

tribute initially to high sediment concentrations in the estuary. As time passes, the sediment concentrations in the estuary basin are gradually reduced because of the seaward transport and deposition process. Much of the deposition occurs in the river channel and the near-shore areas of basin corners. The erosion occurs in the river mouth and the entrance channel areas in which the current velocities are very strong. As the entrainment proceeds into the deeper layers of sediment bed, the erosional rates decrease and thus the suspended-sediment concentrations in the overlying waters are much reduced. The erosional and depositional areas in the estuary are mostly determined by current fields and characteristics of sediment bed.

Flocculation of suspended sediment particles is an important and complex process (Iacobellis, 1984). However, no attempt has been made to model the aggregation and disaggregation of suspended sediments due to the lack of sufficient valid results. This work is presently being done and, in the near future, a preliminary description of flocculation will be included in the model.

ACKNOWLEDGEMENT

This research was supported by the United States Environmental Protection Agency. One of the authors (S.W. Kang) was supported by the UNESCO Fellowships.

REFERENCES

Fukuda, M.K. and W. Lick. 1980. The entrainment of cohesive sediments in fresh water. J. Geophy. Res. **85:** 2813-2824.

Iacobellis, S. 1984. The flocculation of fine-grained lake sediments subjected to a uniform shear stress. M.S. Thesis, University of california, Santa Barbara, CA.

Kang, S.W. 1983. Sediment entrainment due to shear flow. J. Oceanol. Soc. Korea, **18:** 21-28.

Lee, D.Y., W. Lick, and S.W. Kang. 1981. The entrainment and deposition of fine-grained sediments in Lake Erie. J. Great Lakes Res. **7:** 264-275.

Lick, W. 1982. Entrainment, deposition and transport of fine-grained sediments in lakes. Hydrobiologia. **91:** 31-40.

Lick, W. and S.W. Kang. 1986. Entrainment of sediments and dredged materials in shallow lake waters. J. Great Lakes Res., in press.

Massion, G., S.W. Kang, and W. Lick. 1987. Entrainment of uniform-size, fine-grained sediments. J. Great Lakes res., in Press.

Park, Y.A., S.C. Kim, and J.H. Choi. 1986. The distribution and transportation of fine-grained sediments on the inner continental shelf off the Keum River estuary, Korea. J. continental shelf Res. **8:** 499-519.

Tsai, C.H. and W. Lick. 1987. A portable device for measuring sediment resuspension. J. Great Lakes Res., in press.

Wells, J.T., Y.A. Park, and J.H. Choi. 1985. Storm-induced fine-sediment transport, west coast of South Korea. Geo-Marine letters. **4:** 177-180.

Wells, J.T. and O.K. Huh. 1984. Fall-season patterns of turbidity and sediment transport in the Korea Strait and southeastern Yellow Sea. In Ocean Hydrodynamics of the Japan and East China Seas. Elsevier, Amsterdam: 387-397.

Ziegler, C.K. and W. Lick. 1986. A numerical model of the resuspension, deposition, and transport of fine-grained sediments in shallow water. UCSB Report, College of Engineering, University of California, Santa Barbara, CA.

Received January 20, 1987
Accepted March 2, 1987